



A chronopotentiometric approach for measuring chloride ion concentration

Yawar Abbas*, Wouter Olthuis, Albert van den Berg

BIOS-Lab on a Chip Group, MESA+ Institute of Nanotechnology, University of Twente, 7500 AE Enschede, The Netherlands



ARTICLE INFO

Article history:

Received 28 March 2013

Received in revised form 27 May 2013

Accepted 14 July 2013

Available online 23 July 2013

Keywords:

Chloride ion detection

Chronopotentiometry

Stimulus/response approach

Ag/AgCl pseudo-reference electrode

Concrete structures

ABSTRACT

In this paper, a novel approach is reported for the electrochemical measurement of chloride ions in aqueous solution. This sensor is based on the stimulus/response principle of chronopotentiometry. A current pulse is applied at the Ag/AgCl working electrode and the potential change is measured with respect to another identical Ag/AgCl electrode in the bulk electrolyte. The potential difference is related to the Cl^- ion concentration via the Nernst equation and follows an inverse logarithmic trend. By varying the applied current pulse, the sensitivity of the sensor is tunable to different concentration ranges. The potential response is also influenced by the pH of the electrolyte, this effect is pronounced at lower concentration of Cl^- ions ($<1 \text{ mM KCl}$) and at high pH values ($>12 \text{ pH}$). The advantage of this approach is the use of a bare Ag/AgCl electrode as a pseudo-reference electrode, which enables this system for long term application such as the in situ measurement of Cl^- ions in concrete.

© 2013 Elsevier B.V. All rights reserved.

1. Introduction

The major cause of deterioration in reinforcement concrete is due to the presence of chloride ions in the concrete itself [1,2]. When the amount of chloride ions increases beyond a certain threshold, pitting corrosion of the steel reinforcements initiates and ultimately results in localized structural failure [3]. This is particularly a problem in structures near salt water or which are exposed to de-icing salt. In 2011, the U.S.A. Federal Highway Administration stated that 11% of the national bridges are structurally defective [4] mainly due to degradation from chloride ions. Delayed maintenance could result in the collapse of these structures and human casualties, but unnecessary upkeep increases both costs and CO_2 emissions. To precisely predict the optimal time for maintenance of these structures, a service-life model of the concrete is required [5] and the chloride ion concentration is an essential parameter.

The well-established method for chloride ion detection in concrete requires destructive sampling of structures and time-intensive laboratory processing [6,7]. In contrast, a non-destructive in situ monitoring provides fast measurements, data reliability and

real time ingress profile without destroying the structures [8]. In recent years many groups have investigated in situ measurement of chloride in concrete using mainly electrochemical [9–11] and optical methods [12–14]. However, optical methods have bulky setups, are difficult to integrate as a standalone system and have other disadvantages such as the photo bleaching of dyes (optical transducers) and the leaching of transducer (polymer matrix) due to the high pH environment inside concrete.

While electrochemical sensing is the preferred and most researched method, many devices are only suitable for in situ measurements in a laboratory setting and no solution for long-term measurements in concrete structures currently exists (with a required sensing period of 20 years or more). Most of the reported electrochemical sensors use potentiometry [8,11,15–17] where the half-cell potential of a silver/silver chloride (Ag/AgCl) electrode is measured with respect to a reference electrode at equilibrium. This method requires the reference electrode to be embedded inside concrete (near the Ag/AgCl working electrode) to reduce errors due to diffusion potential [18]. The limiting factor of this approach (for in situ measurement in concrete) is the long term stability of the reference electrode and the drift in potential [19]. Therefore, to design an electrochemical sensor capable of measuring a real-time Cl^- ion concentration in concrete over the span of decades, a system that is not dependent on a stable reference electrode is desired.

Potentiometry is a static (zero current) approach and the alternative to this is a dynamic measurement approach (e.g. chronopotentiometry) which involves measuring the response of an equilibrated system to an applied stimulus [20,21]. In this technique, a controlled, chemical stimulus defines the condition at the

Abbreviations: WE, working electrode; RE, reference electrode; CE, counter electrode.

* Corresponding author at: University of Twente, MESA+Institute of Nanotechnology, BIOS chair, Carré 2247, P.O. Box 217, 7500 AE Enschede, The Netherlands. Tel.: +31 053 489 2604.

E-mail addresses: y.abbas@utwente.nl (Y. Abbas), w.olthuis@utwente.nl (W. Olthuis), a.vandenberg@utwente.nl (A. van den Berg).

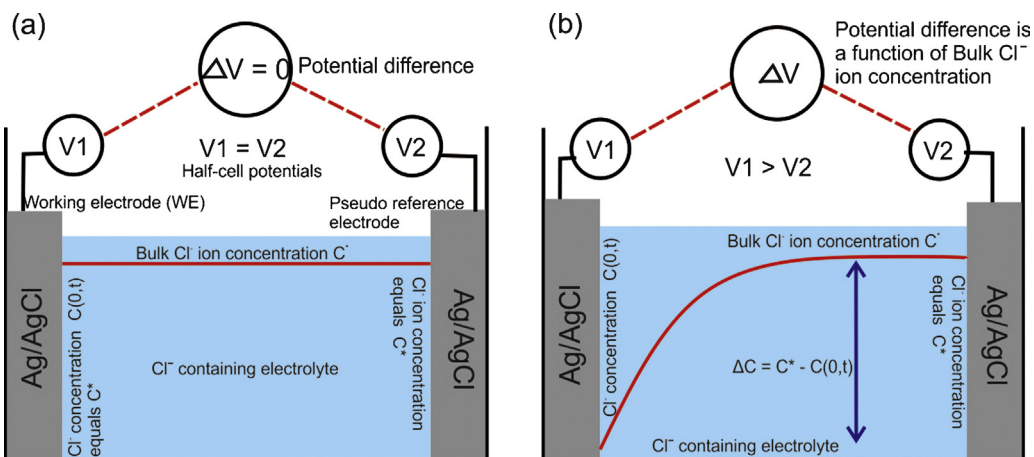


Fig. 1. The schematic of the chronopotentiometric approach with Ag/AgCl as pseudo-reference electrode. (a) At zero current condition, the half-cell potential of the WE and pseudo-reference electrode is the same, therefore the potential difference, ΔV , is zero. (b) During the anodic current pulse at the WE, applied w.r.t. a counter electrode, not included in this figure, the Cl⁻ ions deplete near the WE surface, resulting in a concentration profile w.r.t the bulk electrolyte. The half-cell potential at the WE changes whereas the potential at pseudo-reference electrode remains the same.

working electrode, depending on the analyte concentration (in this case, Cl⁻ ions). A chemical stimulus approach provides improved sensitivity and system robustness by avoiding drift of the potentiometric response [19,22]. Moreover, the dynamic measurement technique can eliminate the dependence of potential measurement on the stable reference electrode.

The aim of this work is to develop a Cl⁻ ion sensor based on chronopotentiometry where the conventional (liquid junction) reference electrode is replaced by a bare Ag/AgCl “pseudo-reference” electrode. A current stimulus is applied at the Ag/AgCl working electrode and the corresponding potential difference is measured simultaneously. This resulting potential difference will vary depending on the Cl⁻ ion concentration in the bulk electrolyte, thereby enabling long-term, in situ measurement of Cl⁻ ions in concrete structures without the need for stable reference electrodes. This method can be used for the in situ measurement of Cl⁻ ions in concrete structures. The theoretical background of this approach along with the experimental evaluation in aqueous solution containing chloride ions are presented in detail.

2. Theory

A Ag/AgCl electrode is a redox electrode of the second kind. When immersed in a solution containing Cl⁻ ions, electrochemical equilibrium occurs between AgCl salt and Cl⁻ ions at the electrode surface, which gives rise to the half-cell potential. The concentration of Cl⁻ ions in the electrolyte determines the half-cell potential, given by the Nernst equation, Eq. (1):

$$V_{\text{Ag/AgCl}} = V^{\circ}_{\text{Ag/AgCl}} - RT/F \ln \alpha_{\text{Cl}^-} \quad (1)$$

Here, $V^{\circ}_{\text{Ag/AgCl}}$, R , F , T , α_{Cl^-} are the standard electrode potential of Ag/AgCl, general gas constant, Faraday constant, absolute temperature (K) and activity of the Cl⁻ ions, respectively. In chronopotentiometry, a constant current is applied at the working electrode (WE) and the potential change is measured with respect to a reference electrode; the measured potential response is called chronopotentiogram. In the case of a Ag/AgCl WE, an anodic current pulse initiates the Faradaic reaction, Eq. (2), at the surface of the WE. The Cl⁻ ions near the WE are consumed during this reaction, locally depleting Cl⁻ ions near the electrode surface [23]. This results in a concentration gradient that gives rise to a potential difference (ΔV) at the WE with respect to the RE. The expression for

ΔV , in the case of high background electrolyte concentration (0.5 M KNO₃) is given in Eq. (3), from the Appendix.



$$\Delta V = -RT/F \ln(1 - \sqrt{(t/D\pi)2j/FC}) \quad (3)$$

Here, C^* is the bulk Cl⁻ ion concentration in the electrolyte, j the current density, t the pulse time and D the diffusion coefficient. Since the potential difference, ΔV , in Eq. (3) does not depend on the reference potential, a bare Ag/AgCl electrode in the bulk electrolyte can serve as a pseudo-reference electrode. The schematic of this approach is shown in Fig. 1. Both Ag/AgCl electrodes are in the same bulk electrolyte. At zero current condition (Fig. 1a), the potential difference is ideally zero (same half-cell potential). During the current pulse (Fig. 1b) applied via a counter electrode (CE), the potential at the WE changes due to the depletion of Cl⁻ ions whereas the half-cell potential of the Ag/AgCl pseudo-reference electrode remains the same. This change in potential, ΔV , is a function of Cl⁻ ion concentration in the bulk electrolyte, as elaborated from Eq. (3).

However, this approach is only valid if the potential difference is measured within the time it takes for the Cl⁻ ion concentration at the electrode surface to reach zero, defined as the transition time (τ) [23]. After the transition time, additional Faradaic reactions occur (e.g. oxide formation) which invalidate Eq. (3). The selection criteria for the current densities, j , and the current-pulse time, t , to ensure measurements within the transition time is outlined in Eq. (4).

$$j < 0.5 FC * \sqrt{(t/D\pi)} \quad (4)$$

This boundary condition is evaluated from the logarithmic-term $(1 - \sqrt{(t/D\pi)2j/FC})$ of Eq. (3). The theoretical curve of this logarithmic-term versus the Cl⁻ ion concentrations of the bulk electrolyte is shown in Fig. 2 for three different current densities. The logarithmic-term values between 0 and 1 give the operational range of this sensor. The sensitivity changes at different values of the Cl⁻ ion concentration. In this work the concentration range of the Cl⁻ ions are selected for values between 0.13 and 0.9 of the logarithmic term to achieve relatively high sensitivity. The sensor then has different sensitivities for specific Cl⁻ ion concentration ranges depending on the applied current density. The detection ranges of Cl⁻ ion concentrations and the corresponding optimal current densities are given in Table 1 for current-pulse time, $t = 5$ s.

The Ag/AgCl electrode is an ion selective electrode which has higher selectivity to Cl⁻ ions than other interfering anions (for instance Br⁻, I⁻, OH⁻ ions) [8]. These interfering ions also contribute

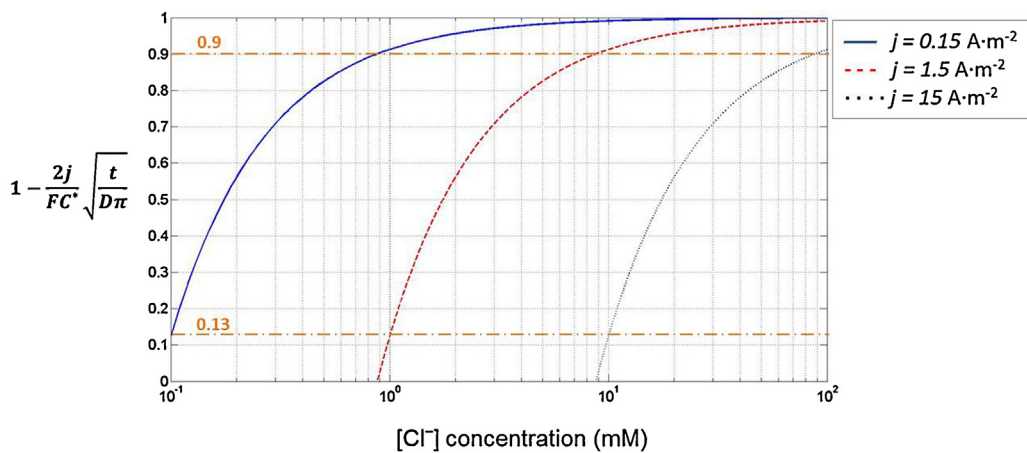


Fig. 2. The theoretical curve of the logarithmic term of Eq. (3) for different current densities versus the Cl^- ion concentrations. The detection range for relatively high sensitivity is defined as the concentration range which corresponds to the values between 0.13 and 0.9 of the logarithmic term.

to the half-cell potential of the Ag/AgCl electrode. The influence of interfering ions is quantified by the selectivity coefficient. For analytical applications the selectivity coefficient of interfering ions is preferably small (ideally zero), but when the interfering ions are more abundant than primary ions this effect becomes more pronounced [8]. In concrete pore solution, the most notable interfering ions are OH^- ions (pH of the electrolyte), which are hydration product from $\text{Ca}(\text{OH})_2$, NaOH and KOH [8]. As long as the ratio of Cl^- to OH^- ions is much greater than the selectivity coefficient, Eq. (5), the effect of pH is trivial. For a Ag/AgCl electrode the selectivity coefficient OH^- ions in aqueous solution, $k_{(\text{Cl}^-, \text{OH}^-)}$, is reported as 2.4×10^{-2} [24].

$$[\text{Cl}^-]/[\text{OH}^-] \gg k_{(\text{Cl}^-, \text{OH}^-)} \quad (5)$$

3. Experimental

3.1. Ag/AgCl electrode fabrication

The Ag/AgCl electrode was fabricated by electro-deposition of silver chloride over a silver wire (0.5 mm dia. and ca. 19.5 mm^2 area). Prior to the electro-deposition, the silver wire was immersed into the acetone bath for 20 min, and then immersed into the concentrated ammonium hydroxide for 2 h to remove any organic contamination and oxide film at the surface, respectively [11,17]. The Ag wire was then chloridized in 0.1 M HCl solution for 20 min at a current density of 13.3 A m^{-2} , to form a AgCl layer (thickness ca. 5 μm) on the surface. The non-anodized area of the electrode was protected through heat shrink tubing. The Ag/AgCl electrode was then stored in 1 M KCl solution.

3.2. Chemicals

The Ag wire ($\geq 99.99\%$ trace metals), potassium chloride (BioXtra, $\geq 99.0\%$), potassium hydroxide (90% pure reagent grade) and potassium nitrate (>99% reagent grade) were ordered from

Sigma-Aldrich, The Netherlands. The KCl and KNO_3 electrolyte solutions were prepared with Milli-Q water.

3.3. Measurement setup

The chronopotentiometric measurements were performed using a VSP potentiostat from Biologic Instruments, France. The WE terminal of the potentiostat was connected to the Ag/AgCl electrode (19.5 mm^2), the reference terminal was connected to another identical Ag/AgCl electrode (pseudo-reference electrode) and the CE terminal was connected to 60 mm^2 Pt counter electrode. The schematic of the measurement setup is shown in Fig. 3. The current pulse is applied between the WE and the CE, and the potential difference, ΔV , of the WE is measured w.r.t to the Ag/AgCl pseudo-reference electrode. The distance between the Ag/AgCl WE and the Pt CE is ca. 1 cm whereas the distance between the WE and the pseudo-reference electrode is ca. 2.5 cm in a glass beaker of 5 mL capacity. All the measurements were performed in a Faraday cage and the measurement parameters were controlled via the user interface of the potentiostat (EC-lab). The pulse time for each

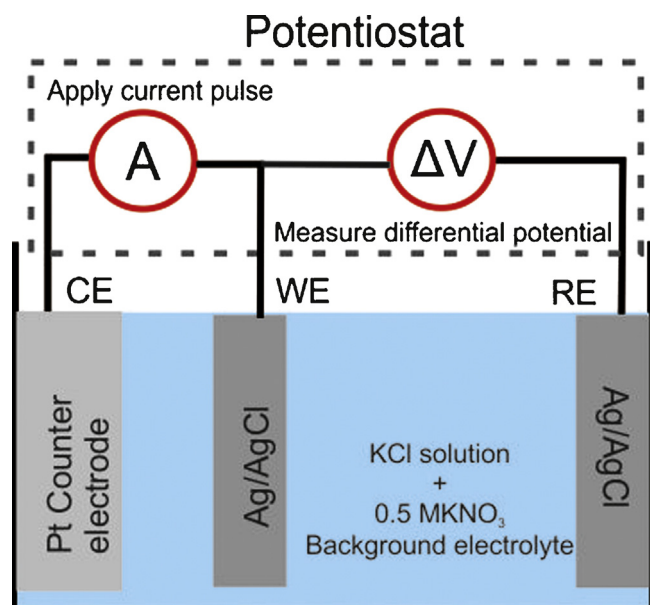


Fig. 3. Schematic representation of the experimental setup for the chronopotentiometric measurements.

Table 1

The selected current densities, j , for different Cl^- ions detection range, at the actuation time of $t = 5 \text{ s}$, elaborated from Eq. (4) and Fig. 2.

No.	$[\text{Cl}^-]$ range (mM)	Current density, j (A m^{-2})
1	0.1–1	0.15
2	1–10	1.5
3	10–100	15

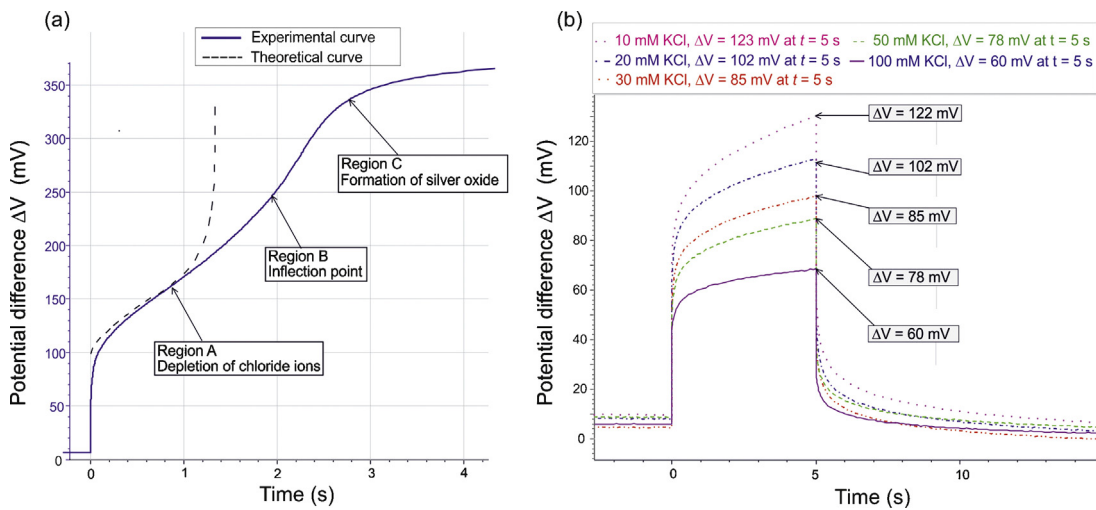


Fig. 4. The potential response of the Ag/AgCl working electrode w.r.t another Ag/AgCl pseudo-reference electrode during the applied current pulse w.r.t a CE, not included in this figure. (a) The experimental and theoretical chronopotentiometric response of the Ag/AgCl WE at a current pulse of 35 A m^{-2} in a 10 mM KCl and 0.5 M KNO_3 bulk electrolyte. (b) The potential difference, ΔV , response for different Cl^- ion concentrations in the bulk electrolyte at 15 A m^{-2} current pulse of 5 s . The ΔV decreases with the increase in Cl^- ion concentration.

applied current was 5 s and the corresponding values of the applied current pulses were derived from Eq. (4). The analytic solutions were composed of various concentrations of KCl in a 0.5 M KNO_3 background electrolyte, and the pH was adjusted by the addition of KOH. All the measurements were carried out at regulated room temperature (22°C).

4. Results and discussions

4.1. Chronopotentiogram of Ag/AgCl electrode

Fig. 4a shows a typical chronopotentiogram of the Ag/AgCl WE electrode w.r.t to another Ag/AgCl electrode in 10 mM KCl solution. Prior to the current pulse, the electrode potential of the Ag/AgCl electrode is ca. 5 mV (ideally zero) due to a nearly identical half-cell potential of the WE and the pseudo-reference electrode in the bulk electrolyte. A current pulse of 35 A m^{-2} is applied at $t=0 \text{ s}$ which results in a rapid ohmic drop of ca. 100 mV . The rate of increase in the potential then slows due to the Cl^- ion depletion near the WE electrode surface, indicated as region A (first plateau) in Fig. 4a. As the Cl^- ions deplete completely near the WE, the slope of ΔV reaches its maximum (region B in Fig. 4a), which corresponds to the transition time. After this point a new plateau (region C in Fig. 4a) is reached (after 2.6 s); this plateau is attributed to the other faradaic reaction, i.e. the formation of silver oxide (Ag_2O). Of these three regions indicated in Fig. 4a, region A is of prime interest as the potential change here is a function of the Cl^- ion concentration. The theoretical curve, based on Eq. (3), is also plotted in Fig. 4a, offset from the initial ohmic drop (100 mV). The transition time measured experimentally is 2.0 s , whereas the theoretical value from Eq. (3) is 1.2 s . This deviation is attributed to the uncertainty in the current density, caused by the roughness of Ag/AgCl electrode surface. The roughness of the Ag/AgCl WE increases the surface area therefore the actual current density is lower than the applied current density. Consequently the transition time, in the experimental curve, is higher than the theoretical one.

Fig. 4b shows the potential response for different Cl^- ion concentrations with an applied current pulse of 15 A m^{-2} . For this current density and concentration range, the current pulse can be applied for 5 s and the potential response still remains within the transition time (region A of Fig. 4a). The ohmic drop at this

current density is in the range of $30\text{--}40 \text{ mV}$. Prior to the current pulse ($t < 0$), the potential difference is nearly zero for all Cl^- ion concentrations. After the applied current pulse ($t > 0$), the potential changes as a function of locally decreasing Cl^- ion concentration; as the number of Cl^- ions in the bulk solution increases, the potential difference between the Ag/AgCl electrode decreases. The potentials are measured at the end of the current pulse ($t = 5 \text{ s}$).

4.2. Calibration curve for chloride ions measurement

Fig. 5 shows the calibration curves for different Cl^- ion concentrations at two current densities: 1.57 and 5.2 A m^{-2} . The theoretical curves from Eq. (3) are also plotted with their respective experimental curves. The experimental curves follow the trend of the theoretical curves, as the potential difference decreases with increasing Cl^- ion concentration. Comparison of the experimental curve with the theoretical one is only relevant for the part of the experimental curve that is on the right hand side of the vertical asymptotic part of the theoretical curve, according to Eq. (4). Only then is the data from region A of Fig. 4a. On the left hand side from this asymptote, silver oxide formation starts to occur (region C in Fig. 4a). As the applied current density increases, the detection window shifts to higher concentrations of Cl^- ions as is evident by the location of the vertical asymptotes in Fig. 5. In the theoretical expression we neglected the ohmic drop due to the high background electrolyte concentration (0.5 M KNO_3). However, there is some ohmic drop which increases with the increase in the applied current pulse.

The Cl^- ion detection range of the sensor is tunable and is a function of the applied current pulse. Fig. 6 shows the calibration curve, measured experimentally, for the particular concentration ranges at the corresponding current densities, given in Table 1. These detection ranges have relatively higher sensitivity at specific current densities as shown in Fig. 2. The corresponding theoretical curves are also plotted in Fig. 6a–c from Eq. (3), at the respective current densities, specified on each curve. The experimental curves in each follow the trend of the theoretical curves, as the potential difference shows an inverse logarithmic response for different Cl^- ion concentrations in the bulk electrolyte. The deviation from the theoretical curve is due to the ohmic drop at high current densities, e.g. in case of Fig. 6b and c the ohmic drop is ca. 30 mV and ca. 55 mV , respectively.

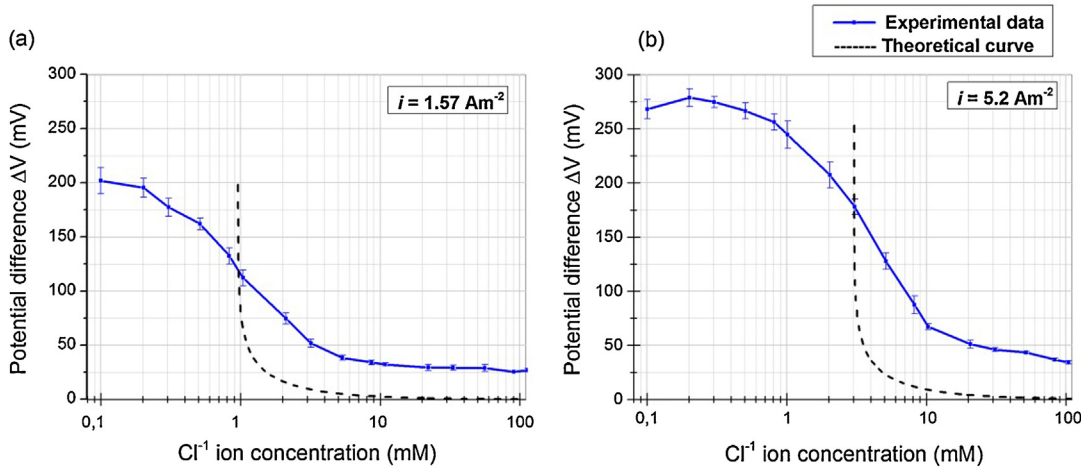


Fig. 5. The theoretical and the experimental calibration curve for different Cl^- ion concentrations at different applied current densities. The electrolyte is composed of different KCl concentration in a 0.5 M KNO_3 solution. For the theoretical curves, $D = 2 \times 10^{-9} \text{ m}^2 \text{ s}^{-1}$ and $T = 22^\circ\text{C}$.

4.3. Effect of the pH

Fig. 7 shows the effect of pH on the measured potential difference at four different Cl^- ion concentrations. In this experiment (Fig. 7), the change in ΔV , for the change in pH of the electrolyte, is investigated and the absolute value of ΔV (at different concentrations) is trivial. The applied current densities are selected according to the condition stated in Eq. (4). Consequently, for the lower concentrations, e.g. 0.1 M KCl, relatively low current density is chosen

(0.1 A m^{-2}), resulting in relatively low ΔV as well as low ohmic drop. Although a decrease in the Cl^- ion concentration increases the potential difference (see Eq. (3)), a decrease in current density along with a lower ohmic drop decreases the potential difference, significantly. The effect of pH is evident at low Cl^- ion concentrations ($[\text{Cl}^-] < 1 \text{ mM}$) for a high pH ($\text{pH} > 12$), see Fig. 7. This is due to the fact that the condition stated in Eq. (5) no longer holds true, e.g. at $0.1 \text{ mM } [\text{Cl}^-]$ and $\text{pH } 12$, $[\text{Cl}^-]/[\text{OH}^-] = 1 \times 10^{-4}/1 \times 10^{-2} = 1 \times 10^{-2}$ is being smaller than $k_{(\text{Cl}^-, \text{OH}^-)}$ (ca. 2.4×10^{-2} , [24]). For this setup,

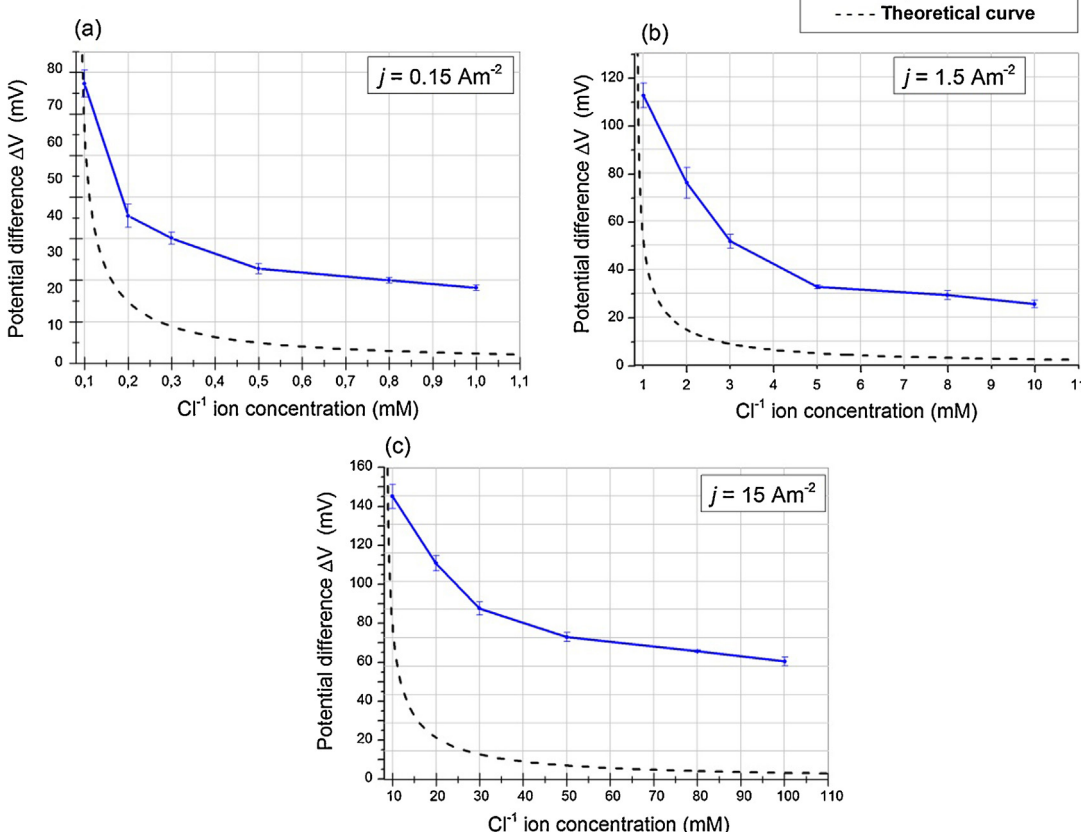


Fig. 6. The calibration curve of the potential difference, ΔV , at different Cl^- ion concentration range. For each concentration range the corresponding current densities, for optimal sensitivity, were calculated from Eq. (4) and given in Table 1.

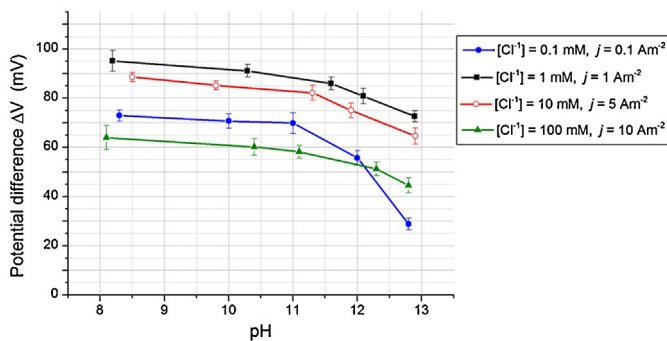


Fig. 7. Effect of pH on the potential difference, ΔV , of the Ag/AgCl electrode. Different current densities were used for different Cl^- ion concentrations of the electrolyte, to satisfy Eq. (4).

the lower detection limit for Cl^- ion concentrations in aqueous solution at $\text{pH} > 12$ is 1 mM. For in situ measurement in concrete this lower detection limit moves to even lower value due to relatively smaller value of $k_{(\text{Cl}^-, \text{OH}^-)}$ inside concrete (ca. 4×10^{-3} , [8]). The change in potential at high pH, for low Cl^- ion concentration, is also attributed to damage of the AgCl membrane from the formation of oxides [8].

5. Conclusion

A chronopotentiometric approach, without a conventional liquid-junction reference-electrode, can be successfully used for the detection of Cl^- ions in aqueous solution. When a current pulse (stimulus) is applied at the Ag/AgCl WE electrode, the change in the electrode potential (response), due to the depletion of Cl^- ions, is a function of Cl^- ion concentration in the bulk electrolyte. In such an approach, a bare Ag/AgCl can serve as a pseudo-reference electrode, enabling this sensor for long term applications. The theoretical expression for the potential difference was derived from the Nernst equation, and the expected inverse logarithmic behavior was observed in experimental measurements. Deviation from the theoretical curve is attributed to the ohmic drop during the applied current pulse. The potential difference for different concentrations of Cl^- ions showed an inverse logarithmic behavior; i.e. the potential decreases with the increase in Cl^- ion concentration. The sensitivity of the response is tunable with the applied current pulse at the corresponding detection range of Cl^- ion concentration. The pH of the electrolyte has an influence on the sensor response. The potential response is not stable at high pH values ($\text{pH} > 12$) for low Cl^- ion concentrations ($< 1 \text{ mM}$). Thus, the lower limit of detection of the Cl^- ion sensor is defined by the pH of the electrolyte and is expected to be even lower when measured inside concrete. We conclude that this measurement approach is very promising to monitor chloride concentrations inside concrete structures.

Acknowledgement

This work is a part of the STW project “Integral solution for sustainable construction (IS2C, <http://is2c.nl/project-10968/>)”. We are grateful to the STW Netherlands for their financial support. We would also like to thank Allison Bidulock for her support during this work.

Appendix A.

Potential response of a Ag/AgCl electrode during an applied current pulse: During the anodic current at the Ag/AgCl WE, the Cl^- ions near the WE are consumed (Faradaic reaction), resulting in a local depletion of Cl^- ions near the electrode surface. The temporal and

spatial gradient of Cl^- ions near the Ag/AgCl electrode, during an applied current pulse, is expressed in Eq. (A.1) [23].

$$C(x, t) = C^* + j(1 - t_{\text{Cl}}^e)/FD\{2\sqrt{(Dt/\pi)}\exp(-x^2/4Dt) - x \operatorname{erfc}[x/2\sqrt{(Dt)}]\} \quad (\text{A.1})$$

Here, C^* is the bulk Cl^- ion concentration in the electrolyte, j the current density, t_{Cl}^e the transport number of Cl^- ion in the electrolyte, x the distance from the electrode surface and D the diffusion coefficient. The expression for the concentration of Cl^- ions at the surface of Ag/AgCl WE ($x=0$) is given in Eq. (A.2), as follows from Eq. (A.1).

$$C(0, t) = C^*(1 - \sqrt{(t/D\pi)}2j(1 - t_{\text{Cl}}^e)/FC^*) \quad (\text{A.2})$$

The applied current pulse and the corresponding concentration gradients give rise to a potential difference (ΔV) at the WE with respect to the reference electrode (RE). This potential difference is the sum of: the ohmic drop due to the impedance of electrolyte ($V_{\Omega,e}$); the growing layer of AgCl salt on the WE ($V_{\Omega,a}$); and, the half-cell electrode potential ($V_{\text{Ag/AgCl}}$) due to the change in Cl^- ion concentration. Therefore:

$$\Delta V = V_{\Omega,e} + V_{\text{Ag/AgCl}} + V_{\Omega,a} \quad (\text{A.3})$$

The ohmic drop, $V_{\Omega,e}$, is contributed by the bulk electrolyte and the diffusion layer near the electrode surface. The half-cell potential, $V_{\text{Ag/AgCl}}$, is given by the Nernst equation. The expression for the overall potential drop, ΔV , at the surface of the Ag/AgCl is expressed by Eq. (A.4) [20].

$$\Delta V = j(d - \sqrt{(\pi Dt)/\lambda C^*} - (\pi t_{\text{Cl}}^e + 1)RT/F \ln(1 - \sqrt{(t/D\pi)}) \times 2j(1 - t_{\text{Cl}}^e)/FC^*) + V_{\Omega,a} \quad (\text{A.4})$$

Here, λ is the conductivity of the electrolyte [$\Omega^{-1} \text{ m}^2 \text{ mol}^{-1}$] and d is the distance between WE and RE. For high background-electrolyte concentration (0.5 M KNO_3), the ohmic drop ($V_{\Omega,e}$) can be neglected, also resulting in a Cl^- ion transport number of $t_{\text{Cl}}^e \approx 0$. The ohmic drop due to the AgCl deposition, $V_{\Omega,a}$, depends on the initial thickness of the AgCl layer. The additional increase in this potential during the current actuation is very small (ca. 1 mV s^{-1}) at a current density of 25 A m^{-2} [20], therefore this potential change can also be neglected. The remaining expression for ΔV is given in Eq. (A.5).

$$\Delta V = -RT/F \ln(1 - \sqrt{(t/D\pi)}2j/FC^*) \quad (\text{A.5})$$

References

- [1] C. Page, K. Treadaway, Aspects of the electrochemistry of steel in concrete, *Nature* 297 (1982) 109–115.
- [2] M. Montemor, A. Simoes, M. Ferreira, Chloride-induced corrosion on reinforcing steel: from the fundamentals to the monitoring techniques, *Cement and Concrete Composites* 25 (2003) 491–502.
- [3] K.Y. Ann, H.W. Song, Chloride threshold level for corrosion of steel in concrete, *Corrosion Science* 49 (2007) 4113–4133.
- [4] Goldmark A. Report one in nine bridges in America structurally deficient, potentially dangerous, <http://transportationnation.org/2011/03/30/2011> [accessed 07.12.12].
- [5] P.D. Cady, R.E. Weyers, Predicting service life of concrete bridge decks subject to reinforcement corrosion, *Corrosion Forms and Control for Infrastructure* 1137 (1992) 328.
- [6] ASTM C-1152, Standard test method for acid-soluble chloride in mortar and concrete, in: Annual Book of ASTM Standard, American Society for Testing Materials, West Conshohocken, PA, USA, 1999.
- [7] T. Rilem, 178-TMC, Recommendation for analysis of total chloride in concrete, *Material and Structures* 35 (2002) 583–585.
- [8] U. Angst, B. Elsener, C.K. Larsen, Ø. Vennesland, Potentiometric determination of the chloride ion activity in cement based materials, *Journal of Applied Electrochemistry* 40 (2010) 561–573.

- [9] R.G. Du, R.G. Hu, R.S. Huang, C.J. Lin, In situ measurement of Cl⁻concentrations and pH at the reinforcing steel/concrete interface by combination sensors, *Analytical Chemistry* 78 (2006) 3179–3185.
- [10] S. Muralidharan, V. Saraswathy, K. Thangavel, N. Palaniswamy, Electrochemical studies on the performance characteristics of alkaline solid embeddable sensor for concrete environments, *Sensors and Actuators B: Chemical* 130 (2008) 864–870.
- [11] M.A. Climent-Llorca, E. Viqueira-Pérez, M.M. López-Atalaya, Embeddable Ag/AgCl sensors for in-situ monitoring chloride contents in concrete, *Cement and Concrete Research* 26 (1996) 1157–1161.
- [12] P.B. Makedonski, Synthesis of New Optical Sensors for Determination of Ph and Chloride Ions in Reinforced Concrete, TU Braunschweig, Braunschweig, Germany, 2004 [dissertation].
- [13] F. Laferrière, D. Inaudi, P. Kronenberg, I.F.C Smith, A new system for early chloride detection in concrete, *Smart Materials and Structures* 17 (2008) 045017.
- [14] V.S. Ban, B.L. Volodin, S. Dolgi, Determination of chloride ion concentrations in concrete by means of near-infrared spectrometry, in: H.F. Wu (Ed.), Non-destructive Characterization for Composite Materials, Aerospace Engineering, Civil Infrastructure, and Homeland Security, SPIE, Bellingham, WA, USA, 2011.
- [15] R. Zielinska, E. Mulik, A. Michalska, S. Achmatowicz, M. Maj-Zurawska, All-solid-state planar miniature ion-selective chloride electrode, *Analytica Chimica Acta* 451 (2002) 243–249.
- [16] F. Cao, D. Greve, I. Oppenheim, Development of microsensors for chloride concentration in concrete, in: Sensors, IEEE, Irvine, CA, 2005, pp. 195–198.
- [17] C. Atkins, J. Scantlebury, P. Nedwell, S. Blatch, Monitoring chloride concentrations in hardened cement pastes using ion selective electrodes, *Cement and Concrete Research* 26 (1996) 319–324.
- [18] U. Angst, Ø. Vennesland, R. Myrdal, Diffusion potentials as source of error in electrochemical measurements in concrete, *Materials and Structures* 42 (2009) 365–375.
- [19] E. Bakker, V. Bhakthavatsalam, K.L. Gemene, Beyond potentiometry: robust electrochemical ion sensor concepts in view of remote chemical sensing, *Talanta* 75 (2008) 629–635.
- [20] P. Bergveld, J. Eijkel, W. Olthuis, Detection of protein concentrations with chronopotentiometry, *Biosensors and Bioelectronics* 12 (1997) 905–916.
- [21] W. Olthuis, P. Bergveld, Integrated coulometric sensor-actuator devices, *Microchimica Acta* 121 (1995) 191–223.
- [22] S. Makarychev-Mikhailov, A. Shvarev, E. Bakker, Calcium pulstrodes with 10-fold enhanced sensitivity for measurements in the physiological concentration range, *Analytical Chemistry* 78 (2006) 2744–2751.
- [23] A.J. Bard, L.R. Faulkner, *Electrochemical Methods: Fundamentals and Applications*, 2nd ed., John Wiley, New York, 2001.
- [24] Y. Umezawa, *CRC Handbook of Ion-Selective Electrodes: Selectivity Coefficients*, CRC Press, Boca Raton, FL, 1990.

Biographies

Yawar Abbas received his MSc degree in microsystem engineering from Department of Microsystem Engineering, IMTEK, University of Freiburg, Germany in 2011. During his master thesis he worked on the development of an active microfluidic mixer in a PDMS chip using Braille pin actuator, at Chair of MEMS application. Since December 2011 he has been working on his PhD at the BIOS group, MESA+ Institute of Nanotechnology, University of Twente, the Netherlands. The main goal of his PhD project is the in situ measurement of chloride ions in concrete structures, in collaboration with Microlab TU Delft (the Netherlands) and TPM group TU Eindhoven (the Netherlands).

Wouter Olthuis received his MSc degree in electrical engineering from the University of Twente, Enschede, The Netherlands in 1986. In that year, he joined the Center for Microelectronics, Enschede (CME). In 1987 he started his PhD project and received the PhD degree from the Biomedical Engineering Division of the Faculty of Electrical Engineering, University of Twente, in 1990. Since 1991 he has been working as an assistant professor in the Laboratory of Biosensors, part of the MESA+ Research Institute, of the University of Twente and as such co-supervising many projects on both physical and (bio)chemical sensors and sensor systems for medical and environmental applications. Currently, he is an associate professor in the BIOS Lab-on-Chip group of the MESA+ Institute of Nanotechnology and is as such responsible for the theme electrochemical sensors and sensor systems. From 2006 until 2011 he was also the Director of the Educational Program of Electrical Engineering at the Faculty of Electrical Engineering, Mathematics and Computer Science at the University of Twente.

Albert van den Berg received his MSc in applied physics in 1983, and his PhD in 1988 both at the University of Twente, the Netherlands. From 1988–1993 he worked in Neuchatel, Switzerland, at the CSEM and the University (IMT) on miniaturized chemical sensors. From 1993 until 1999 he was research director Micro Total Analysis Systems (μ TAS) at MESA, University of Twente. In 1998 he was appointed as part-time professor “biochemical analysis systems”, and later in 2000 as full professor on miniaturized systems for (bio)chemical analysis in the faculty of Electrical Engineering. He received several honors and awards such as Simon Stevin (2002), ERC advanced grant (2008), Spinoza prize (1009) and honorary university professorship (2010). He has co-authored over 220 papers ($H=36$) and over 10 patents, and has been involved in >5 spin-off companies. His current research interests focus on microanalysis systems and nanosensors, nanofluidics and single cells and tissues on chips, especially with applications in personalized health care and development of sustainable (nano)technologies.